RSC Advances

PAPER

View Article Online
View Journal | View Issue

Cite this: *RSC Adv.*, 2023, **13**, 1985

A novel reaction mechanism for the synthesis of coconut oil-derived biopolyol for rigid poly(urethane-urea) hybrid foam application

Roger G. Dingcong, Jr, *[a] Roberto M. Malaluan,[ab] Arnold C. Alguno,[a] Dave Joseph E. Estrada,[a] Alona A. Lubguban,[c] Eleazer P. Resurreccion,[d] Gerard G. Dumancas,[e] Harith H. Al-Moameri[f] and Arnold A. Lubguban *[ab]

Coconut oil (CO) has become one of the most important renewable raw materials for polyol synthesis due to its abundance and low price. However, the saturated chemical structure of CO limits its capability for functionalization. In this study, a novel reaction mechanism *via* the sequential glycerolysis and amidation of CO triglycerides produced an amine-based polyol (p-CDEA). The synthesized biopolyol has a relatively higher hydroxyl value of 361 mg KOH per g relative to previously reported CO-based polyols with values ranging from 270–333 mg KOH per g. This primary hydroxyl-rich p-CDEA was used directly as a sole B-side polyol component in a polyurethane-forming reaction, without further purification. Results showed that a high-performance poly(urethane-urea) (PUA) hybrid foam was successfully produced. It has a compressive strength of 226 kPa and thermal conductivity of 23.2 mW (m^{-1} K^{-1}), classified as type 1 for a rigid structural sandwich panel core and type 2 for rigid thermal insulation foam applications according to ASTM standards. Fourier-transform infrared (FTIR) spectroscopy was performed to characterize the chemical features of the polyols and foams. Scanning electron microscopy (SEM) analysis was also performed to evaluate the morphological structures of the synthesized foams. Differential scanning calorimetry (DSC) and thermogravimetric analysis (TGA) were conducted to investigate the foam's thermal characteristics. Thus far, this work is the first to report a novel and effective reaction mechanism for the synthesis of a highly functional CO-derived polyol and the first CO-based polyol with no petroleum-based replacement that may serve as raw material for rigid PUA foam production. PUA hybrid foams are potential insulation and structural materials. This study further provided a compelling case for enhanced sustainability of p-CDEA PUA hybrid foam against petroleum-based polyurethane.

Received 26th October 2022
Accepted 31st December 2022

DOI: 10.1039/d2ra06776e

rsc.li/rsc-advances

1. Introduction

Polyurethane (PU) is one of the most versatile polymeric materials with a wide range of industrial applications such as thermal rigid insulation foam, flexible foam, coatings, adhesives, elastomers, *etc.*[1–4] Its application depends on its properties, which are highly influenced by the type of polyol and isocyanate used in its production.[1,5,6] Conventional PUs are derived from non-renewable fossil fuels.[2,7–9] However, industrial-scale production of these non-biodegradable substances poses significant environmental hazards.[10,11] The rapid rate of fossil fuel depletion compels research institutions and PU manufacturing industries to explore alternative feedstocks such as vegetable oils that are sustainable, renewable, and eco-friendly.[3,12–17]

Biopolyols are the potential alternative raw materials for the sustainable production of rigid PU foam, but in order to do so, polyols would require a relatively high hydroxyl value.[18] Vegetable oils do not naturally contain hydroxyl groups and are less suitable reactants in polyols production than other substrates unless chemical modifications are made.[19] Hydroxyl groups are therefore chemically generated from vegetable oils, the number of which is dependent on the nature and triglyceride structure of the specific oil. Unsaturated vegetable oils are typically modified by double bond epoxidation and ring-opening reactions with alcohols and haloacids.[6,7,20] Saturated vegetable oils usually undergo transesterification and amidation reactions.[12,21–24] However, previous studies on saturated

[a]*Center for Sustainable Polymers, Mindanao State University – Iligan Institute of Technology, Iligan City 9200, Philippines. E-mail: arnold.lubguban@g.msuiit.edu.ph*
[b]*Department of Chemical Engineering and Technology, Mindanao State University – Iligan Institute of Technology, Iligan City 9200, Philippines*
[c]*Department of Mathematics, Statistics, and Computer Studies, University of the Philippines Rural High School, Paciano Rizal, Bay, Laguna 4033, Philippines*
[d]*Civil Engineering Technology, Montana State University-Northern, Havre, MT 59501, USA*
[e]*Department of Chemistry, The University of Scranton, Scranton, PA 18510, USA*
[f]*Materials Engineering Department, Mustansiriyah University, Baghdad 10052, Iraq*

vegetable oil modification reported polyols with low hydroxyl values, which necessitates petroleum-based polyol replacement to be effective for use in rigid PU foam formation.[25,26] This major limitation is attributed to the mostly unsaturated composition of vegetable oil triglycerides making it less capable of hydroxyl functionalization.[7]

Philippines is the second-largest coconut producer in the world next to Indonesia.[27] It is reported that the country's annual coconut production is estimated at an average of 14.5 metric tons from 2011 to 2020 on about 3.3 million hectares of coconut farms, nearly 30% of the country's total farmlands.[28,29] With this abundance and the opportunity for value addition in the coconut supply chain, research on CO as a raw material for rigid PU foam production is warranted.

In this study, a highly functional biopolyol (p-CDEA) derived from CO and diethanolamine (DEA) was synthesized *via* sequential glycerolysis and amidation reactions. The chemical and structural properties of the synthesized polyol were characterized based on its hydroxyl (OH) value, amine (NH) value, viscosity, and functional groups using Fourier-transform infrared (FTIR) spectroscopy. The autocatalytic effect of p-CDEA in a PU-forming reaction was also investigated by varying its substitution in the PU foam formulation where gel and cream times were measured. The resulting poly(urethane-urea) (PUA) hybrid foams' mechanical properties were characterized according to their compressive strength, thermal conductivity, and density. The morphological features and thermal properties of the PU foam samples were characterized using scanning electron microscopy (SEM), differential scanning calorimetry (DSC), and thermogravimetric analysis (TGA), respectively.

2. Materials and methods

2.1. Materials and methods

Refined, bleached, and deodorized (RBD) CO was obtained from a local coconut processing facility. Polymeric methylene diphenyl diisocyanate (PAPI™ 27 from Dow Chemical, has an NCO functionality and content of 2.7 and 31.4 wt%, respectively), calcium oxide (CaO), zinc oxide (ZnO), silicone surfactants (INV 690 and Dabco DC 2585), catalyst (Polycat® 8), petroleum-based polyether polyol (Voranol® 490 from Dow Chemical, has an alcohol functionality of 4.3, an average molecular weight of 460, and a hydroxyl number of 490), and refined glycerol were provided by Chemrez Technologies. Reagent-grade diethanolamine [$NH_2(C_2H_4OH)_2$] (DEA) was provided by Ajax Finechem and reagent-grade hydrochloric acid (HCl) and methyl red was purchased from Sigma-Aldrich.

2.2. Glycerolysis of CO

Glycerolysis of CO was done in a closed Parr reactor with automated temperature control and agitator. A previously optimized glycerolysis reaction was carried out using a CO and glycerol weight ratio of 6 : 1 with 0.05 wt% CaO catalyst at 215 °C for 2 hours.[30] A clear yellowish liquid product comprising mostly of monoglycerides (MG), as the ideal product, and a fraction of diglycerides (DG) and triglycerides (TG), which are collectively denoted as C-GRD, was produced.[30]

2.3. Catalytic amidation of C-GRD

Amidation of C-GRD was carried out using the same Parr reactor at various reaction times (0–5 h) and weight ratios of DEA to C-GRD (0.02–0.13) with 0.15 wt% ZnO catalyst. The reaction temperature was maintained at 140 °C.[23] A dark yellow biopolyol (p-CDEA) was produced following the general amidation pathways of C-GRD described in Fig. 3.

2.4. Preparation of rigid poly(urethane-urea) foam

A modified rigid PU foam formulation described by Tu *et al.* (2007) was used in this study with the components outlined in Table 1.[31] The A-side component used in the formulation is polymeric Methyl Diphenyl Diisocyanate (MDI) added to the B-side at an isocyanate index of 110. B-side reactants comprising polyol(s), surfactants, blowing agent, and catalyst were weighed into a 500 mL disposable plastic cup and mixed at 3450 rpm for 10–15 s. The mixture was degassed for 120 s, and then PAPI™ 27 polymeric MDI was rapidly added with continuous stirring for another 10–15 s at a similar speed. The mixture was immediately poured into a wooden mold ($11.4 \times 11.4 \times 21.6$ cm^3) with an aluminum foil lining, and the foam was allowed to rise and set under ambient conditions (23 °C, 1 atm). The cream times and gel times were recorded to investigate p-CDEA's catalytic effect during the foaming process. The synthesized PUA foams were labeled according to the type and level of polyol substitution (*i.e.*, fossil-based polyol = Voranol® 490 and CO-based polyol = p-CDEA). A PU-V490 labeled foam has no p-CDEA in its formulation (*i.e.*, completely fossil-based) while a PU-p-CDEA foam has none of the Voranol® 490 (*i.e.*, completely bio-based). Further, PU-40-p-CDEA and PU-80-p-CDEA foams have 40 wt% p-CDEA-60 wt% Voranol®490 and 80 wt% p-CDEA-20 wt% Voranol®490 polyols in their formulation, respectively. Two types of surfactants were also used in combination with the different p-CDEA formulations. The prepared foam samples were allowed to cure for seven days before characterization.

2.5. Analyses of polyols

The synthesized polyol's hydroxyl and total amine values were measured according to ASTM D4274-16 test method D and ASTM D2074-92, respectively.[32,33] The rotational viscosity of the samples was measured according to ASTM D4878-15 using a Brookfield DV3T rheometer (AMETEK Brookfield, Middleborough, MA) maintaining a torque ranging from 30% to 40% and a temperature of 50 ± 0.1 °C.[34] The p-CDEA samples' functional groups were evaluated using a Shimadzu IR Tracer 100 (Shimadzu Corp., Kyoto, Japan) spectrometer. A total of 40 scans from each sample at wavelengths between 4000 to 400 cm^{-1} were obtained at a resolution of 2 cm^{-1}.

Table 1 Poly(urethane-urea) foam formulation at different p-CDEA substitutions

Foam formulation	Components	PU-V490 (no p-CDEA)	PU-40-p-CDEA	PU-80-p-CDEA	PU-p-CDEA (no Voranol® 490)
Polyol	p-V490	100	60	20	0
	p-CDEA	0	40	80	100
Catalyst	Polycat 8	1.75	1.75	1.75	1.75
Surfactant	INV 690	3	3	3	3
	Dabco DC 2585	3	3	3	3
Blowing agent	Water	2	2	2	2
Isocyanate	MDI PAPI™ 27	144.94	131.40	117.87	111.10

2.6. Characterization of poly(urethane-urea) hybrid foams

The thermal conductivity of each PU foam sample was tested using a FOX 200 heat flow meter (Laser-Comp, Wakefield, MA) according to ASTM C518-2017 (sample size 150 × 150 × 20 mm).[35] The densities of the foam samples were determined according to ASTM D1622-03.[36] Compressive strengths of foam samples were measured with a Universal Testing Machine Shimadzu AGS-X Series (Shimadzu Corp., Kyoto, Japan) according to ASTM D1621-04a.[37] The thermal transitions of the prepared foams were evaluated through differential scanning calorimetry (DSC) using a PerkinElmer DSC 4000 (PerkinElmer, Waltham, MA) with a heating rate of 10 °C minute^{-1} (sample weight 5–10 mg).[25] Thermogravimetric analysis (TGA) was carried out using a Shimadzu DTG 60H (Shimadzu Corp., Kyoto, Japan) under a nitrogen atmosphere with a heating rate of 10 °C from 45 °C to 800 °C (sample weight 5–10 mg). The morphological features of the foams' surfaces were evaluated through scanning electron microscopy (SEM) using a JEOL JSM-6510LA SEM (JEOL, Ltd, Tokyo, Japan).

3. Results and discussions

3.1. Chemical properties of glycerides and p-CDEA

CO is composed of triglycerides (TG) or triacylglycerols having three saturated fatty acids esterified in a glycerol backbone.[18] The glycerolysis reaction of CO, shown in Fig. 1 involves breaking down its triglyceride structure using glycerol as the source of nucleophile (electron donor). The resulting products are composed of MG, DG, unreacted TG, and traces of free fatty acids (FFA).[2]

The chemical composition or functional groups present in CO, C-GRD, and p-CDEA were analyzed through their characteristic IR spectra as shown in Fig. 2. A broad peak at 3359 cm^{-1} in the C-GRD spectrum represents the presence of hydroxyl moieties in C-GRD.[30] This peak confirms the generation of hydroxyl functionality during the conversion of less functional CO into a hydroxyl-functionalized C-GRD. A sharp peak at 1733 cm^{-1} represents the carbonyl stretching absorption band indicating the presence of ester carbonyl bonds in all three samples. A significant difference in carbonyl peak intensity can be observed with CO and C-GRD. This implies the conversion of triglycerides into di- and mono-glycerides during the glycerolysis of CO.[38] The fatty acid chain structure is revealed by the combined peaks located at 2922 cm^{-1} and 2853 cm^{-1} which is expected for CO and retained for both C-GRD and p-CDEA.

The prepared C-GRD samples were characterized for their hydroxyl values. The results showed an average value of 253 mg KOH per g of sample, which fails to comply with the hydroxyl number requirement for rigid PU foam application at 350–800 mg KOH per g.[18] This limitation in the glycerolysis process warrants the use of DEA to effectively increase the OH-functionality in C-GRD. DEA, with the characteristic primary hydroxyl group in its structure, was chemically introduced into C-GRD *via* amidation reaction producing the amine-based p-CDEA polyol.

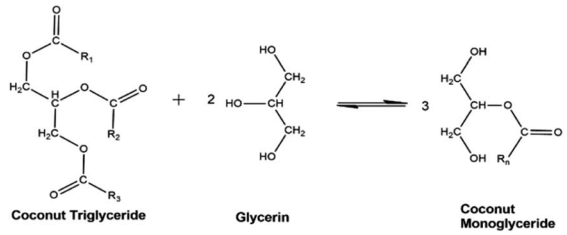

Fig. 1 Ideal glycerolysis reaction of coconut triglyceride with monoglyceride as major reaction product.

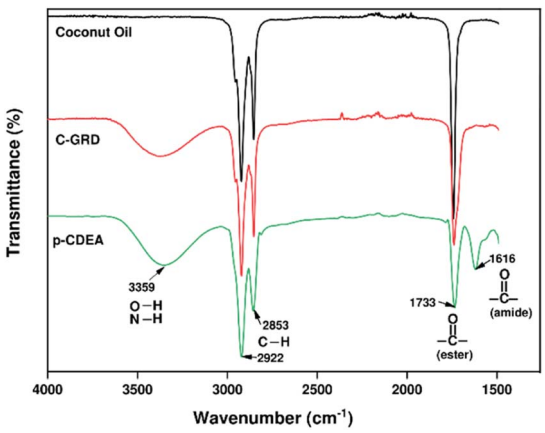

Fig. 2 FTIR spectra of coconut oil (CO), synthesized glycerides (C-GRD), and biopolyol (p-CDEA) showing their characteristic fatty acid chains, reduction of carbonyl concentration as functionalization proceeds, and verification of amide formation in p-CDEA.

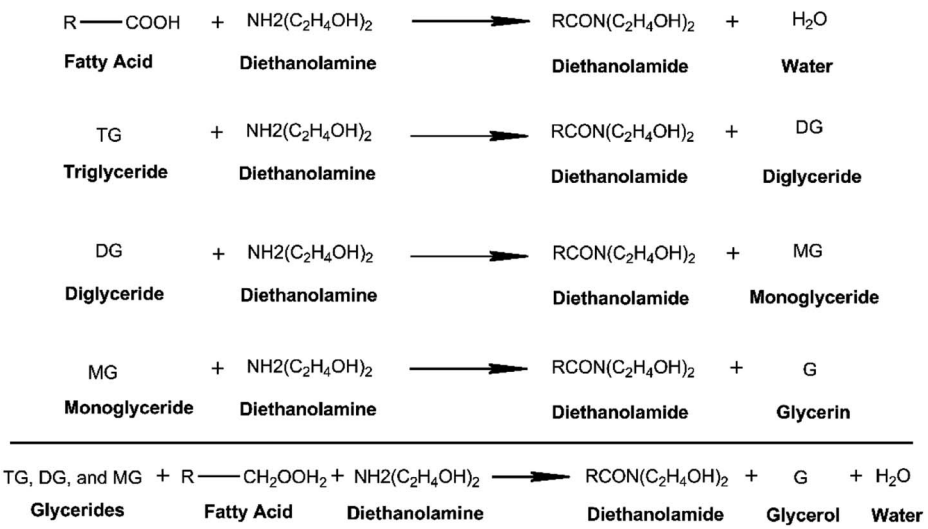

Fig. 3 General amidation pathway of alkyl-substituted glycerides and free fatty acids (FFAs) using diethanolamine with ideal products – diethanolamide, glycerol, and water.

Fig. 3 shows the general amidation pathways and the overall net reaction between ester-containing glycerides and DEA. Amidation of C-GRD with DEA involves the breaking of the ester bonds of all glycerides forming diethanolamide and glycerol.[12,18,39–41] Simultaneously, FFA can also react with DEA to yield diethanolamide and traces of water.[40] The FTIR spectra of p-CDEA in Fig. 2 reveal an amide carbonyl band centered at 1616 cm^{-1}, indicative of the presence of an amide carbonyl bond. This strongly confirms the formation of diethanolamide in the amidation products.

The amidation reaction was evaluated at different DEA/C-GRD mass ratios and characterized by its viscosity and hydroxyl value, as shown in Fig. 4. A significant increase in the hydroxyl value was observed for DEA/C-GRD mass ratios of 0.02–0.11, as shown in Fig. 4a. The hydroxyl moieties present in the excess DEA. On the other hand, the increasing addition of DEA showed no significant changes in the polyol's viscosity, as shown in Fig. 4b. This implies that the amidation of C-GRD with DEA does not yield a long-chain polyol.

ZnO was previously used as a structural base catalyst for chemoselective amidation of aliphatic carboxylic acid.[42] It acts as an activating agent of the acyl group assisting hydrogen ion transfer during the amidation reaction. To investigate the effect of ZnO as an amidation catalyst for CO, parallel catalytic and non-catalytic amidation reactions were conducted. The resulting p-CDEA sample products were characterized for their hydroxyl values, as shown in Fig. 5. It was observed that both reaction types yield p-CDEA polyols with close hydroxy values at higher reaction times (≥250 minutes). Stabilization of the polyol hydroxyl values indicates the completion of the amidation reaction. Based on the results, catalytic amidation of C-GRD hastened the rate of reaction and reached its completion relatively much earlier compared to the non-catalyzed reaction. The hydroxyl values of p-CDEA started to stabilize at 180 min for the

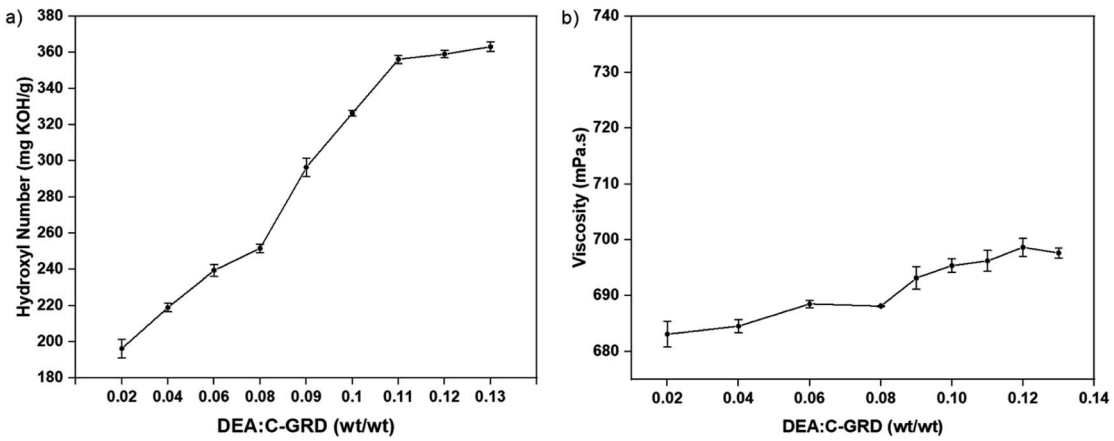

Fig. 4 (a) Hydroxyl value and (b) viscosity behavior of biopolyol (p-CDEA) at different diethanolamine (DEA) loadings in coconut glycerides (C-GRD).

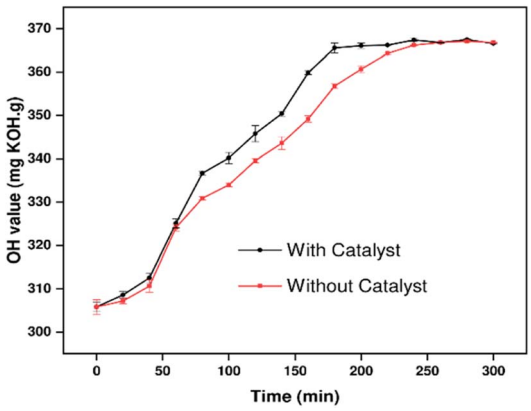

Fig. 5 Hydroxyl values catalytic (using 0.15 wt% ZnO) and non-catalytic amidation of coconut glycerides (C-GRD) at 140 °C for 3 hours.

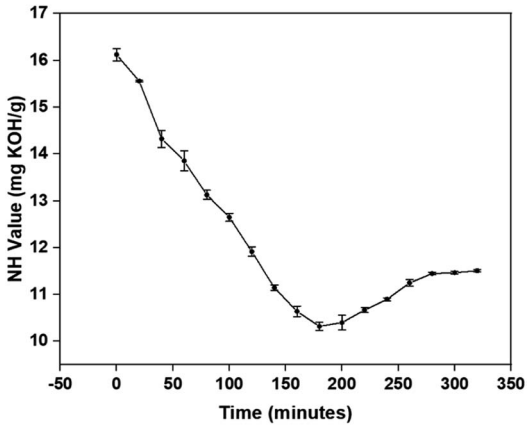

Fig. 7 Effect of reaction time on the amine (NH) value of biopolyol (p-CDEA).

catalyzed amidation and 260 min for the non-catalyzed reaction. Suitable hydroxyl values (in the range of 350–380 mg KOH per g) of p-CDEA were attained for both catalyzed (using 0.15 wt% ZnO) and non-catalyzed complete amidation of C-GRD at 140 °C. These results indicated that catalytic amidation significantly reduced reaction energy by increasing the rate of reaction. This translates to a more economical and sustainable polyol processing should production is increased to an industrial scale.

Ideally, the amidation reaction of coconut MG with DEA would yield diethanolamide and glycerol.[12] However, Stirna *et al.* (2011, 2012) reported an equilibrium between diethanolamide and fatty acid amino esters as shown in Fig. 6.[23,24] The IR signals of p-CDEA at 1616 cm^{-1} and 1733 cm^{-1} shown in Fig. 2 corresponded to the presence of an amide and ester carbonyl bonds which are structural features of diethanolamide and amino ester, respectively.[43] These observed peaks verify the presence of amino ester in equilibrium with diethanolamide. Hence, p-CDEA also contains secondary amine moieties present in the amino ester components.

The equilibrium conversion of amine moieties of p-CDEA into an amide can be observed through the NH values at different reaction times as shown in Fig. 7. The lowest NH value was achieved at 180 min, corresponding to the reaction time for the complete stoichiometric conversion of C-GRD into p-CDEA *via* amidation. From this optimum reaction time (180 min), the slight increase and eventual stabilization of the NH value as the reaction time increases (up to 340 min) can be attributed to the formation of amino esters in equilibrium with diethanolamide.[23,24] The NH moieties present in the amino esters would also react with isocyanates forming urea bonds that contribute to the polymer cross-linking that makes up the hard segments of the polymer structure.[44–46]

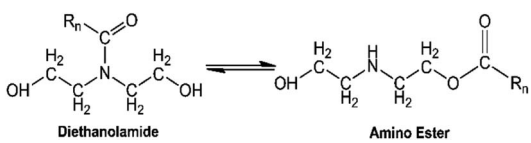

Fig. 6 Structure of coconut fatty acid diethanolamide in equilibrium with amino esters.

3.2. Poly(urethane-urea) (PUA) foam synthesis and properties

The physicochemical properties of the prepared PUA foam samples were characterized to evaluate the potential of the synthesized polyol for rigid foam application. PUA foams were produced (Table 1) using the optimized p-CDEA polyol, catalytically synthesized with 0.15 wt% ZnO, a DEA/C-GRD mass ratio of 0.11, and processed at 140 °C for 180 min. PUA foam synthesis consisted of two simultaneous reactions: gelling and blowing reactions. Typical foam formulations use different types of catalysts for gelling and blowing, which are both amine-based. However, the foaming formulation in p-CDEA does not include a blowing catalyst since p-CDEA is an amine hybrid that manifests an autocatalytic effect during the reaction of water and isocyanate.[47]

The autocatalytic effect of p-CDEA was investigated by evaluating the gel and cream times of the PUA reaction, as shown in Fig. 8. There was a significant decrease in both gel and cream times of the PUA foam reactions as p-CDEA substitution was increased. As suggested earlier, this faster reaction rate is due to

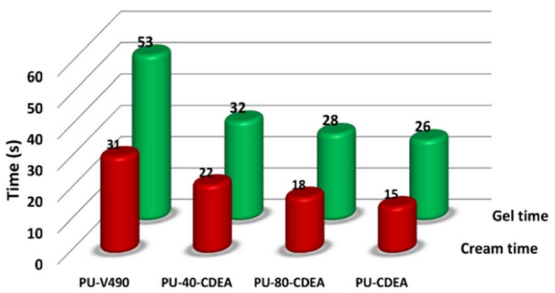

Fig. 8 Comparative reaction gel and cream times of the control fossil-based foam (PU-V490) and different biopolyol (p-CDEA)-substituted poly(urethane-urea) PUA hybrid foam formulations.

the presence of intrinsic amine moieties existing in p-CDEA. Its catalytic effect accelerates the reaction between water and isocyanate and promotes faster bubble size expansion. Simultaneously, the presence of relatively short-chain molecules in p-CDEA such as free glycerol decelerates polymer chain propagation thereby reducing the cell resistance towards the accelerated bubble expansion.[25] As a result, significant ripped cells were observed in the prepared PUA foam (Fig. 9) as p-CDEA substitution increased.

Fig. 10 shows the FTIR spectra of the methylene and carbonyl groups of the synthesized PUA hybrid foams at different p-CDEA substitutions in the formulation. As the level of p-CDEA concentration increases, the peak intensities around 2926 cm^{-1} and 2856 cm^{-1} also increase. This is indicative of the increasing abundance of methylene groups attributed to the coconut fatty acid chains of p-CDEA. Hybrid PUA foam formation was confirmed of having ester carbonyl and amide carbonyl bands at around 1717 cm^{-1} and 1607 cm^{-1}, respectively. These carbonyl groups are characteristic features of both urethane and urea compounds.

The thermal properties of the prepared foams were investigated through DSC as shown in Fig. 11. A significant thermal transition of PU-V490 thermograms can be found in the range of 14 °C–80 °C. These transition temperatures reveal the

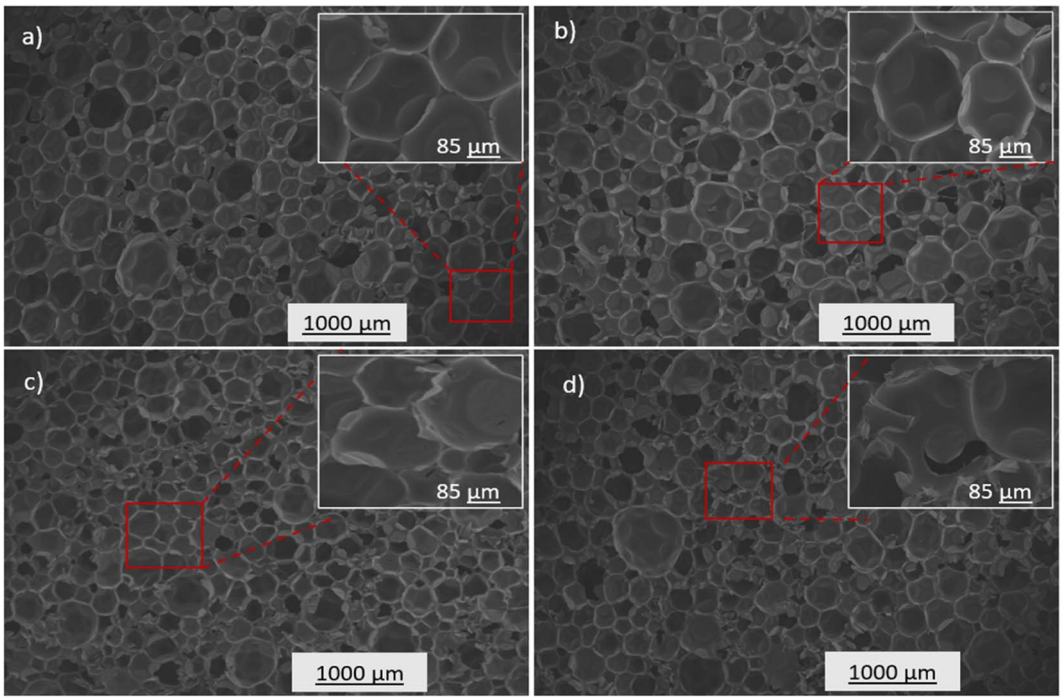

Fig. 9 SEM micrographs of the cell structures of the control (a) Fossil-based (PU-V490) and different biopolyol (p-CDEA)-substituted poly(-urethane-urea) (PUA) foams: (b) 40% biopolyol substituted foam (PU-40-p-CDEA), (c) 80% biopolyol substituted foam (PU-80-p-CDEA), and (d) 100% biopolyol substituted foam (PU-p-CDEA). An increasing foam cell disorder was observed as p-CDEA substitution is increased in the PUA hybrid foam formulation.

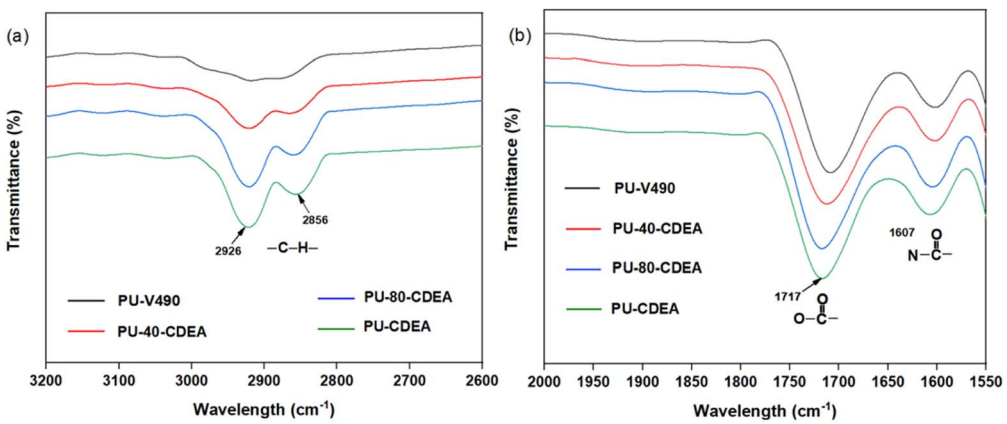

Fig. 10 FTIR spectra of (a) methylene and (b) carbonyl functional groups of the poly(urethane-urea) (PUA) hybrid foams.

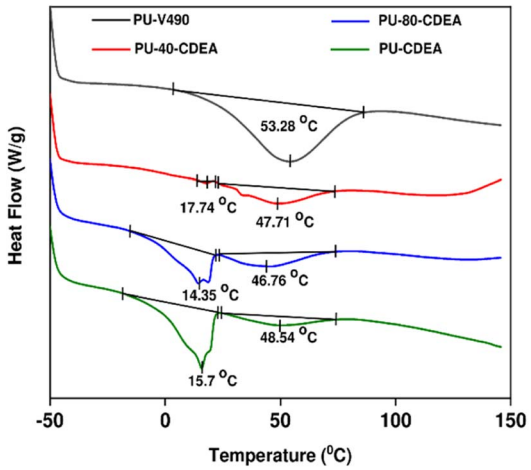

Fig. 11 DSC plot of poly(urethane-urea) (PUA) hybrid foams showing enthalpy changes corresponding to the effect of different levels of urea and urethane concentrations.

dissociation of hydrogen bonds which occurs at the glass transition temperature of urethane segments.[25] Similar thermal transitions can also be observed for all PUA foam samples. The enthalpy changes at these transition temperatures also decrease with increasing p-CDEA substitution. One reason for this is the decreasing urethane concentration in the foam samples. Moreover, p-CDEA-substituted foam samples reveal a unique thermal transition ranging from −17 °C–20 °C, vastly different from the PU-V490 control. This transition might be attributed to the glass transition temperatures of urea segments[48] which in Fig. 11 showed a consistently increasing enthalpy change as p-CDEA concentration is increased in the foam formulation. These observations reveal the coexistence of urethane and urea bonds in the foams incorporated with p-CDEA polyol.

The thermal decomposition pattern of the prepared foams is shown in Fig. 12. PU-V490 reveals two endothermic peaks at around 314 °C and 535 °C (Fig. 12a). The first peak corresponded to the thermal decomposition of urethane and allophanate bonds while the second peak corresponded to the thermal decomposition of the polyol chains.[49–51] In contrast, PU-p-CDEA exhibits multiple degradation peaks (Fig. 12d). The first two degradation peaks at 151 °C and 265 °C corresponded to the thermal decomposition of urea and urethane hard segments, respectively.[40] This relatively lower degradation temperature of the foams associated with p-CDEA substitution demonstrates lower thermal stability in the PUA foams. Furthermore, the third and fourth peaks at 419 °C and 543 °C were indicative of the degradation of soft segments of urea and urethane bonds, respectively.[40] The presence of multiple degradation peaks in both PU-40-p-CDEA and PU-80-p-CDEA shown in Fig. 12b and c, respectively, could be attributed to the combined compositional effects of p-V490 and p-CDEA.

The influence of p-CDEA polyol addition on the physical and mechanical properties such as compressive strength and thermal conductivity of the PUA foam is shown in Table 2. The structural features of the foam highly influence the compressive strength of the prepared PUA hybrid foams. Increasing the level of p-CDEA concentration in the foam formulation also increases the occurrence of ripped, irregular cell structures (Fig. 9) owing to the relatively high reaction rates of the PUA formation.[25] Relative to the regular foam cell morphology of PU-V490, the presence of ripped cells in the substituted PUA foams reduces the structural integrity thereby reducing their compressive strengths.

Table 2 shows that the increasing p-CDEA substitution yields PUA foams with relatively lower compressive strength and higher thermal conductivity. Despite PU-p-CDEA having the

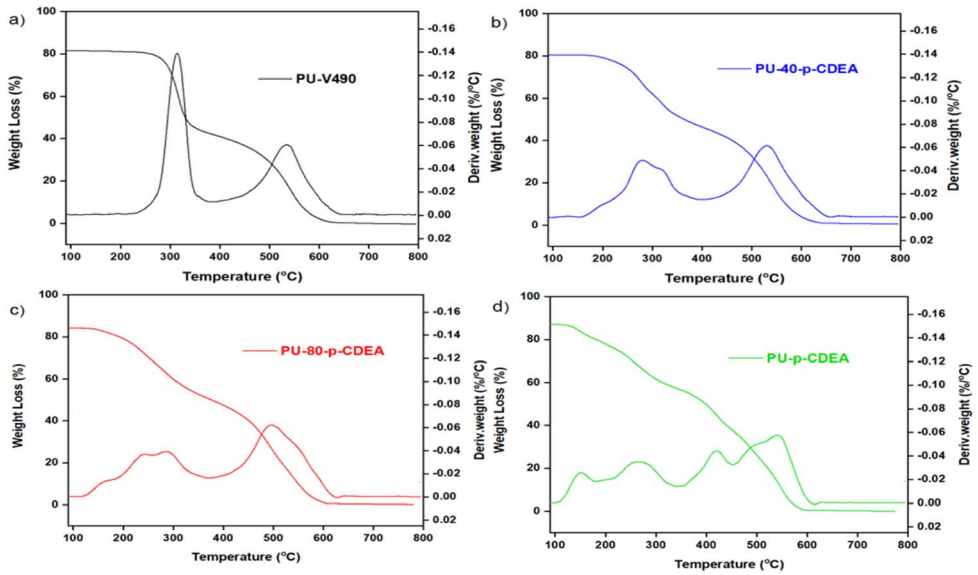

Fig. 12 DTG curves of poly(urethane-urea) PUA hybrid foams at different biopolyol (p-CDEA) substitutions – (a) 100% petroleum-based polyol (PU-V490), (b) 40% CO-based polyol substitution (PU-40-p-CDEA), (c) 80% CO-based polyol substitution (PU-80-p-CDEA), and (d) 100 CO-based polyol substitution (PU-p-CDEA).

Table 2 Mechanical and insulative properties of poly(urethane-urea) PUA hybrid foams at different biopolyol (p-CDEA) polyol substitutions

Properties	PU-V490	PU-40-p-CDEA	PU-80-p-CDEA	PU-p-CDEA
Compressive strength, (kPa) (vertical to foam rise)	723 ± 15	357 ± 15	285 ± 15	226 ± 15
Thermal conductivity, [mW (m^{-1} K^{-1})]	21.6 ± 0.3	22.0 ± 0.3	22.6 ± 0.3	23.2 ± 0.3
Density, kg m^{-3}	46.1 ± 1.5	42.3 ± 1.3	38.5 ± 1.4	37.6 ± 1.2

Table 3 ASTM standard properties for structural sandwich panel and thermal insulation polyurethane foams

	ASTM E-1730		ASTM C-1029	
Properties	Type I	Type II	Type 1	Type II
Compressive strength, min (kPa)	≥172.4	≥275.8	≥104.0	≥173.0
Thermal conductivity, max [mW (m^{-1} K^{-1})]	≤36.0	≤37.0	≤23.5	≤23.5

lowest compressive strength of 226 kPa, it nevertheless satisfies the standard compressive strength required for rigid structural and thermal insulation applications. The increasing thermal conductivities corresponding to the increasing p-CDEA substitution might be attributed to the increasing amount of PUA ripped cell structures, which translates to the formation of open foam cell morphology as shown in Fig. 9.[49,50] These open cells in the PUA foams offer less resistance to heat transfer thus promoting lesser insulative capacity. Nevertheless, all thermal conductivities of the PUA foams including the wholly substituted PU-p-CDEA (*i.e.*, no petroleum-based p-V490 polyol added) still comply with the established ASTM standards for all types of insulating foams.

4. Conclusions

In this study, the synthesis of an amine-based polyol p-CDEA from CO *via* subsequent glycerolysis and amidation reactions was explored. The resulting polyol exhibited a relatively high hydroxyl value of 361 mg KOH per g (compared to a previously reported CO-based polyol) and an amine value of 10.32 mg KOH per g. Catalytic amidation (using 0.15 wt% ZnO) reduces the energy consumption in the polyol-forming reaction of C-GRD operating at a relatively lower temperature of 140 °C to complete the reaction as confirmed by FTIR analysis. This translates to a more economical and sustainable polyol processing in a large-scale setup. Poly(urethane-urea) (PUA) hybrid rigid foams were successfully produced using different levels of replacement of the petroleum-based Voranol® 490 polyol by the bio-based p-CDEA polyol. Thermal analysis *via* DSC indicated the coexistence of urethane and urea bonds in the foams incorporated with p-CDEA polyol. TGA revealed the thermal decomposition of urea and urethane's hard and soft segments shown as multiple degradation peaks in p-CDEA-substituted hybrid foams. The lower degradation temperatures of the foams associated with p-CDEA substitution imply lower thermal stability as the p-CDEA concentration in the foam formulation is increased. This is also confirmed by the increasing occurrence of ripped foam cells (shown in the hybrid foams' SEM analysis) as the level of p-CDEA is increased. Moreover, the hybrid foams' mechanical and insulative properties characterization results showed that a high-performance foam, with a compressive strength of 226 kPa and thermal conductivity of 23.2 mW (m^{-1} K^{-1}), can be achieved up to 100% p-CDEA replacement in the foam formulation. According to ASTM standards shown in Table 3, this foam (PU-p-CDEA) can be used for type I rigid structural sandwich panel core and type II rigid thermal insulation foam applications. The success of this study showed the improvement in the polyol-forming functionalization techniques for CO using a novel reaction mechanism of modifying the sequence of established reactions aided by catalytic action to reduce the process energy requirement. In addition, this work successfully produced rigid PUA hybrid foams with full bio-based polyol replacement that complies with ASTM standards on structural and rigid thermal insulation. The results of this study present potential impacts on PU industries' sustainable initiatives: raw materials, contribution to climate change, circularity, impacts on the environment and human health, and product quality.

Author contributions

Roger Dingcong Jr: methodology, investigation, analysis, figure preparation, writing, review, and editing. Dave Joseph Estrada: analysis, methodology. Roberto Malaluan: supervision (lead), investigation, analysis, writing, review, and editing. Alona Lubguban: statistical analysis. Eleazar Resurreccion: writing, review, and editing. Gerard Dumancas: review and editing. Harith AL-Moameri: review and editing. Arnold Lubguban: supervision (lead), investigation, analysis, writing, review, and editing. All authors have given approval for the final version of the manuscript.

Conflicts of interest

There are no conflicts of interest to declare.

Acknowledgements

The authors would like to acknowledge the financial support of the Philippine Council for Industry, Energy and Emerging

Technology Research and Development (PCIEERD) of the Department of Science and Technology (DOST) through the Niche Centers in the Region (NICER) – R&D Center for Sustainable Polymers.

Notes and references

1 F. M. De Souza, P. K. Kahol and R. K. Gupta, Introduction to Polyurethane Chemistry, *ACS Symp. Ser.*, 2021, **1380**, 1–24, DOI: 10.1021/bk-2021-1380.ch001.

2 K. W. O. N. Soon-Ki and S. K. C. Kil-Yeong Choi, Synthesis and Properties of Polyurethanes and Polyureas Containing 2,5-Thiophenylene Linkage, *Brevity*, 2014, **25**, 198–213, DOI: 10.1093/acprof:oso/9780199664986.003.0012.

3 L. J. Lee, C. Zeng, X. Cao, X. Han, J. Shen and G. Xu, Polymer nanocomposite foams, *Compos. Sci. Technol.*, 2005, **65**(15–16), 2344–2363, DOI: 10.1016/j.compscitech.2005.06.016.

4 Y. Yanping, The development of polyurethane, *Mater. Sci. Mater. Rev.*, 2018, **1**(1), 1–8, DOI: 10.18063/msmr.v1i1.507.

5 S. Gopalakrishnan and T. Linda Fernando, Influence of polyols on properties of bio-based polyurethanes, *Bull. Mater. Sci.*, 2012, **35**(2), 243–251, DOI: 10.1007/s12034-012-0279-5.

6 X. Li, Z. Fang, X. Li, S. Tang, K. Zhang and K. Guo, Synthesis and application of a novel bio-based polyol for preparation of polyurethane foams, *New J. Chem.*, 2014, **38**(8), 3874–3878, DOI: 10.1039/c4nj00600c.

7 Z. S. Petrovic, Polyurethanes from vegetable oils, *Polym. Rev.*, 2008, **48**(1), 109–155, DOI: 10.1080/15583720701834224.

8 M. Ionescu, *Chemistry and Technology of Polyols for Polyurethanes*, 2005.

9 M. Ionescu and Z. S. Petrović, High Functionality Polyether Polyols Based on Polyglycerol, *J. Cell. Plast.*, 2010, **46**(3), 223–237, DOI: 10.1177/0021955X09355887.

10 J. B. Mariano and E. R. L. Rovere, *Environmental impacts of the oil industry. Encycl Life Support Syst*, 2017, pp. 1–6, https://www.eolss.net/Eolss-SampleAllChapter.aspx.

11 M. A. P. Langone, M. E. De Abreu, M. J. C. Rezende and G. L. Sant'anna, *Appl. Biochem. Biotechnol.*, 2002, **98**, 987–996.

12 T. A. Patil, Amidation of lanolin and Amidation of Vegetable Oils for Rust Preventive Coatings Application, *Int. J. Adv. Sci. Tech. Res.*, 2016, **1**(6), 504–512.

13 U. A. Amran, K. M. Salleh, S. Zakaria, *et al.*, Production of rigid polyurethane foams using polyol from liquefied oil palm biomass: Variation of isocyanate indexes, *Polymers*, 2021, **13**(18), 1–20, DOI: 10.3390/polym13183072.

14 P. K. Renjith, C. Sarathchandran, V. Sivanandan Achary, N. Chandramohanakumar and V. Sekkar, Micro-cellular polymer foam supported silica aerogel: Eco-friendly tool for petroleum oil spill cleanup, *J. Hazard. Mater.*, 2021, **415**, 1–10, DOI: 10.1016/j.jhazmat.2021.125548.

15 S. Członka and A. Strąkowska, Rigid Polyurethane Foams Based on Bio-Polyol and Additionally Reinforced with Silanized and Acetylated Walnut Shells for the Synthesis of Environmentally Friendly Insulating Materials, *Materials*, 2020, **13**(15), 3245, DOI: 10.3390/ma13153245.

16 S. A. Gurusamy-Thangavelu, S. J. Emond, A. Kulshrestha, *et al.*, Polyurethanes based on renewable polyols from bioderived lactones, *Polym. Chem.*, 2012, **3**(10), 2941–2948, DOI: 10.1039/c2py20454a.

17 D. S. Kaikade and A. S. Sabnis, Polyurethane foams from vegetable oil-based polyols: a review, *Polym. Bull.*, 2022, 1–23, DOI: 10.1007/s00289-022-04155-9.

18 P. Furtwengler and L. Avérous, Renewable polyols for advanced polyurethane foams from diverse biomass resources, *Polym. Chem.*, 2018, **9**(32), 4258–4287, DOI: 10.1039/c8py00827b.

19 G. Soto, A. Castro, N. Vechiatti, F. Iasi, A. Armas, N. E. Marcovich and M. A. Mosiewicki, *Polym. Test.*, 2017, **57**, 42–51.

20 A. A. Lubguban, R. J. G. Ruda, R. H. Aquiatan, *et al.*, Soy-Based Polyols and Polyurethanes, *KIMIKA*, 2017, **28**(1), 1–19, DOI: 10.26534/kimika.v28i1.1-19.

21 L. Yuan, Z. Wang, N. M. Trenor and C. Tang, Amidation of triglycerides by amino alcohols and their impact on plant oil-derived polymers, *Polym. Chem.*, 2016, **7**(16), 2790–2798, DOI: 10.1039/c6py00048g.

22 C. W. Cheung, M. L. Ploeger and X. Hu, Direct amidation of esters with nitroarenes, *Nat. Commun.*, 2017, **8**, 11161–11172, DOI: 10.1038/ncomms14878.

23 U. Stirna, A. Fridrihsone, M. Misane and D. Vilsone, Rapeseed Oil as Renewable Resource for Polyol Synthesis, *Environ Clim Technol*, 2011, **6**(1), 85–90, DOI: 10.2478/v10145-011-0012-4.

24 U. Stirna, B. Lazdiņa, D. Vilsone, *et al.*, Structure and properties of the polyurethane and polyurethane foam synthesized from castor oil polyols, *J. Cell. Plast.*, 2012, **48**, 476–488, DOI: 10.1177/0021955X12445178.

25 X. Leng, C. Li, X. Cai, *et al.*, A study on coconut fatty acid diethanolamide-based polyurethane foams, *RSC Adv.*, 2022, **12**(21), 13548–13556, DOI: 10.1039/d2ra01361d.

26 A. Paruzel, S. Michałowski, J. Hodan, P. Horák, A. Prociak and H. Beneš, Rigid Polyurethane Foam Fabrication Using Medium Chain Glycerides of Coconut Oil and Plastics from End-of-Life Vehicles, *ACS Sustainable Chem. Eng.*, 2017, **5**(7), 6237–6246, DOI: 10.1021/acssuschemeng.7b01197.

27 M. L. Moreno, J. K. M. Kuwornu and S. Szabo, Overview and Constraints of the Coconut Supply Chain in the Philippines, *Int. J. Fruit Sci.*, 2020, **20**(S2), S524–S541, DOI: 10.1080/15538362.2020.1746727.

28 C. T. Lim, Forecasting coconut production in the Philippines with ARIMA model, *AIP Conf. Proc.*, 2015, **1643**, 86–92, DOI: 10.1063/1.4907429.

29 R. T. Dy and S. Reyes, *The Philippine Coconut Industry : Performance , Issues And Recommendations*, Philippines, 2006, pp. 1–8.

30 T. N. Mehta and S. N. Shah, Glycerolysis of coconut, sesame, and linseed oils. Fractionation of the products with alcohol and urea, *J. Am. Oil Chem. Soc.*, 1957, **34**(12), 587–591, DOI: 10.1007/BF02638759.

31 Y.-C. Tu, P. Kiatsimkul, G. Suppes and F.-H. Hsieh, *J. Appl. Polym. Sci.*, 2007, **105**, 453.

32 ASTM Standard D4274, *Standard Test Methods for Testing Polyurethane Raw Materials: Determination of Hydroxyl Number of Polyols*, ASTM International, West Conshohocken, PA, 2016, **https://www.astm.org**.

33 ASTM Standard D2074, *Standard Test Methods for Total, Primary, Secondary, and Tertiary Amine Values of Fatty Amines by Alternative Indicator Method*, ASTM International, West Conshohocken, PA, 2019, **https://www.astm.org**.

34 ASTM Standard D4878, *Standard Test Methods for Polyurethane Raw Materials: Determination of Viscosity of Polyols*, ASTM International, West Conshohocken, PA, 2016, **https://www.astm.org**.

35 ASTM Standard C518, *Standard Test Method for Steady-State Thermal Transmission Properties by Means of the Heat Flow Meter Apparatus*, ASTM International, West Conshohocken, PA, 2021, **https://www.astm.org**.

36 ASTM Standard D1622, *Standard Test Method for Apparent Density of Rigid Cellular Plastics*, ASTM International, West Conshohocken, PA, 2003, **https://www.astm.org**.

37 ASTM Standard D1621, *Standard Test Method for Compressive Properties of Rigid Cellular Plastics*, ASTM International, West Conshohocken, PA, 2004, **https://www.astm.org**.

38 J. J. Mueller, S. Baum, L. Hilterhaus, M. Eckstein, O. Thum and A. Liese, Simultaneous determination of mono-, di-, and triglycerides in multiphase systems by online Fourier transform infrared spectroscopy, *Anal. Chem.*, 2011, **83**(24), 9321–9327, DOI: **10.1021/ac2018662**.

39 D. Kumar, S. M. Kim and A. Ali, One step synthesis of fatty acid diethanolamides and methyl esters from triglycerides using sodium doped calcium hydroxide as a nanocrystalline heterogeneous catalyst, *New J. Chem.*, 2015, **39**(9), 7097–7104, DOI: **10.1039/c5nj00388a**.

40 H. P. Das, T. S. V. R. Neeharika, C. Sailu, V. Srikanth, T. P. Kumar and K. N. P. Rani, Kinetics of amidation of free fatty acids in jatropha oil as a prerequisite for biodiesel production, *Fuel*, 2017, **196**, 169–177, DOI: **10.1016/j.fuel.2017.01.096**.

41 G. Li, C. L. Ji, X. Hong and M. Szostak, Highly Chemoselective, Transition-Metal-Free Transamidation of Unactivated Amides and Direct Amidation of Alkyl Esters by N-C/O-C Cleavage, *J. Am. Chem. Soc.*, 2019, **141**(28), 11161–11172, DOI: **10.1021/jacs.9b04136**.

42 F. Tamaddon, F. Aboee and A. Nasiri, ZnO nanofluid as a structure base catalyst for chemoselective amidation of aliphatic carboxylic acids, *Catal. Commun.*, 2011, **16**(1), 194–197, DOI: **10.1016/j.catcom.2011.09.023**.

43 P. S. Kalsi, *Spectroscopy of Organic Compounds*, New Age International (P) Ltd, New Delhi, 2004, pp. 65–184.

44 R. F. Rekker WTN, *The Reaction of Hydroxy-Esters and Amino-Esters with Isocyanates*, 2010, vol. 15, iss 2, pp. 1–23.

45 D. J. Primeaux II, *Polyurea vs. Polyurethane & Polyurethane/Polyurea: What's the Difference*, 2004.

46 J. Dodge, *Polyurethanes and Polyureas*, 2003, DOI: **10.1002/0471220523**.

47 F. M. De Souza, P. K. Kahol and R. K. Gupta, Introduction to Polyurethane Chemistry, *ACS Symp. Ser.*, 2021, **1380**, 1–24, DOI: **10.1021/bk-2021-1380.ch001**.

48 G. Toader, A. Diacon and E. Rusen, *et al.*, *A Facile Synthesis Route of Hybrid Polyurea-Polyurethane-MWCNTs Nanocomposite Coatings for Ballistic Protection and Experimental Testing in Dynamic Regime Gabriela*, 2021.

49 R. Tanaka, S. Hirose and H. Hatakeyama, Preparation and characterization of polyurethane foams using a palm oil-based polyol Ryohei, *Bioresour. Technol.*, 2008, **99**(9), 3810–3816, DOI: **10.1016/j.biortech.2007.07.007**.

50 I. Zagożdżon, P. Parcheta and J. Datta, Novel cast polyurethanes obtained by using reactive phosphorus-containing polyol: Synthesis, thermal analysis and combustion behaviors, *Materials*, 2021, **14**(11), 1–18, DOI: **10.3390/ma14112699**.

51 R. Gu, M. Khazabi and M. Sain, Fiber reinforced soy-based polyurethane spray foam insulation. Part 2: Thermal and mechanical properties, *BioResources*, 2011, **6**(4), 3775–3790.